Climate warming leads to divergent succession of grassland microbial communities

Xue Guo[1,2,3,4,11], Jiajie Feng[2,3,11], Zhou Shi[2,3,11], Xishu Zhou[1,2], Mengting Yuan[2,3,5], Xuanyu Tao[2,3], Lauren Hale[2,3], Tong Yuan[2,3], Jianjun Wang[2,3], Yujia Qin[2,3], Aifen Zhou[2,3], Ying Fu[2,3], Liyou Wu[2,3], Zhili He[2,3], Joy D. Van Nostrand[2,3], Daliang Ning[2,3,4], Xueduan Liu[1] , Yiqi Luo[3,6,7], James M. Tiedje[8], Yunfeng Yang[2,4]* and Jizhong Zhou[2,3,4,9,10]*

[1]School of Minerals Processing and Bioengineering, Central South University, Changsha, China. [2]Institute for Environmental Genomics, University of Oklahoma, Norman, OK, USA. [3]Department of Microbiology and Plant Biology, University of Oklahoma, Norman, OK, USA. [4]State Key Joint Laboratory of Environment Simulation and Pollution Control, School of Environment, Tsinghua University, Beijing, China. [5]Department of Environmental Science, Policy, and Management, University of California, Berkeley, CA, USA. [6]Center for Ecosystem Science and Society, Department of Biological Sciences, Northern Arizona University, Flagstaff, AZ, USA. [7]Department of Earth System Science, Tsinghua University, Beijing, China. [8]Center for Microbial Ecology, Michigan State University, East Lansing, MI, USA. [9]School of Civil Engineering and Environmental Sciences, University of Oklahoma, Norman, OK, USA. [10]Earth and Environmental Sciences, Lawrence Berkeley National Laboratory, Berkeley, CA, USA. [11]These authors contributed equally: Xue Guo, Jiajie Feng, Zhou Shi. *e-mail: yangyf@tsinghua.edu.cn; jzhou@ou.edu

Accurate climate projections require an understanding of the effects of warming on ecological communities and the underlying mechanisms that drive them[1–3]. However, little is known about the effects of climate warming on the succession of microbial communities[4,5]. Here we examined the temporal succession of soil microbes in a long-term climate change experiment at a tall-grass prairie ecosystem. Experimental warming was found to significantly alter the community structure of bacteria and fungi. By determining the time-decay relationships and the paired differences of microbial communities under warming and ambient conditions, experimental warming was shown to lead to increasingly divergent succession of the soil microbial communities, with possibly higher impacts on fungi than bacteria. Variation partition- and null model-based analyses indicate that stochastic processes played larger roles than deterministic ones in explaining microbial community taxonomic and phylogenetic compositions. However, in warmed soils, the relative importance of stochastic processes decreased over time, indicating a potential deterministic environmental filtering elicited by warming. Although successional trajectories of microbial communities are difficult to predict under future climate change scenarios, their composition and structure are projected to be less variable due to warming-driven selection.

The acceleration of global climate warming, a consequence of the build-up of atmospheric CO_2 and other greenhouse gases due to fossil fuel combustion

and land use change, represents one of the greatest scientific and policy concerns in the twenty-first century[1]. As climate, especially temperature, is a primary driver of biological processes[6], climate warming has impacted terrestrial biodiversity at all system levels[7,8], including shifting species' geographical range[7], phenology[8], distribution and abundance[7], all of which could potentially increase the risk of extinction[9], altering community structure[10] and disrupting ecological interactions and ecosystem functioning[11]. Consequently, it is anticipated that climate warming will alter patterns in spatial and temporal distributions of organisms[12]. However, despite intensive studies examining the responses of ecological communities to climate warming[13], whether and how climate warming affects temporal succession of ecological communities, particularly microbial communities, remains elusive.

As knowledge of the temporal dynamics of ecological communities is critical for predicting the responses of biodiversity, ecosystem functions and services to environmental change (for example, climate warming), ecological succession has always been at the core of community ecology[10,14]. Stages, trajectories and mechanisms are central topics in successional studies[14]. The succession of ecological communities can be convergent, divergent, idiosyncratic or other complex forms in linear or nonlinear fashions[14,15]. Previous studies showed that plant successions were divergent[16], convergent[16–18] or showed no significant change[17], and sometimes all patterns appeared within the same study[18]. Moreover, successional direction could be dependent on both spatial and temporal scales[16,19], ecosystem characteristics[19], types of perturbation[19], and functional traits used[20]. However, only a few studies examined temporal succession in microbial communities, and those showed convergent[21] or divergent[19,22,23] behaviours.

In the last decades, various manipulated, multifactorial, climate change, field experiments have been established[10,13,18,24], and offer unique opportunities for examining the temporal succession of terrestrial ecosystems in response to climate change across multiple environmental conditions. Therefore, in this study, we examined the temporal succession of soil microbial communities in response to experimental warming in a native, tall-grass prairie ecosystem of the US Great Plains in Central Oklahoma (34° 59′N, 97° 31′W)[24]. This long-term multifactor climate change experiment was established in 2009, and the warming treatment plots have been subjected to continuous +3 °C warming by infrared radiators[24]. In this report, we primarily focus on the warming effects on microbial community succession by determining: whether and how warming will alter temporal succession rates of the grassland soil microbial communities across different organismal groups (for example, bacteria and fungi); whether warming will lead to divergent or convergent succession of soil microbial communities; and what the relative roles of deterministic and stochastic processes are in shaping temporal succession of soil microbial communities in response to climate warming.

Table 1: Significance tests of the effects of experimental warming on the microbial community structure across six years with three different statistical approaches

Data sets	Adonis		ANOSIM		MRPP	
	F	*P*	*R*	*P*	*δ*	*P*
Bacteria (16S)	2.611	**0.004**	0.097	**0.004**	0.489	**0.004**
Fungi (ITS)	2.005	**0.001**	0.129	**0.001**	0.861	**0.001**

All three tests are non-parametric multivariate analyses based on Bray–Curtis dissimilarities among samples, including the permutational multivariate analysis of variance (Adonis), analysis of similarity (ANOSIM) and multiple response permutation procedure (MRPP). For Adonis, only the warming effect is shown above, and the other terms are shown in Supplementary Table 1. For ANOSIM and MRPP, the permutation was constrained within each block in each year by setting 'strata' in the functions ANOSIM and MRPP in the R package vegan. Significant *P* values (<0.005) are shown in bold.

Over the last six years, the average temperature in the surface soil was significantly ($P < 0.01$) increased by 2.8 °C and soil moisture was decreased by 12.2% in the warmed plots (Supplementary Fig. 1a,b). Consistent with our previous study[24,25,26], some key ecosystem processes including gross primary productivity (GPP), ecosystem respiration (ER), soil total respiration (TR) and heterotrophic respiration (HR) were significantly ($P < 0.05$) altered by experimental warming (Supplementary Fig. 1c,d). The concentrations of soil nitrate significantly ($P < 0.05$) increased, but soil total nitrogen, total organic carbon, ammonia and soil pH remained unchanged under warming (Supplementary Fig. 1e,f).

It is expected that the alterations in soil variables and plant productivity in response to warming would lead to changes in microbial communities over time. To test this hypothesis, a total of 48 surface soil (0–15 cm) samples taken annually from 2009 to 2014 from 4 replicate plots, under warming and control (ambient) conditions, were analysed using amplicon-based sequencing of 16S ribosomal RNA genes for bacteria and archaea, and internal transcribed spacers (ITSs), for fungi. An average of $53{,}000 \pm 26{,}000$ and $23{,}000 \pm 11{,}000$ sequence reads per sample were obtained for the 16S rRNA gene and ITS, respectively. The microbial community structures of bacteria and fungi were altered over time by warming, as visualized by the non-metric multidimensional scaling ordination based on the Bray–Curtis dissimilarity (Supplementary Fig. 2). Specifically, the close clustering of warmed and control samples in 2009 indicated similar soil microbial composition and structures of bacteria and fungi before warming treatment. In the subsequent years, the warmed samples were generally separated from the control samples on a yearly basis (Supplementary Fig. 2). Moreover, three complementary non-parametric multivariate statistical tests (Adonis, ANOSIM and MRPP) further revealed that the overall microbial community structures of bacteria and fungi across all years were significantly different

($P < 0.05$) between the warmed and control plots (Table 1 and Supplementary Table 1). These results indicated that experimental warming significantly altered soil bacterial and fungal community composition and structure.

To understand the impacts of warming on the temporal turnovers of microbial community structure, the time-decay relationships (TDRs) of soil bacteria and fungi were measured based on taxonomic diversity by a linear regression between log-transformed community similarity and log-transformed temporal distance[27]. Since different facets of diversity could behave quite differently[28], we also examined the TDRs based on phylogenetic diversity, wherein the genetic relatedness of organisms in an environment is taken into account along with species richness and relative abundance[28]. The slopes of the linear regression, TDR value (v), can reflect the temporal turnover rates of soil microbes. Our results first revealed that under ambient temperature there were no significant TDRs based on either taxonomic or phylogenetic diversity for bacteria (Fig. 1a,c), but there were significant TDRs with relatively small temporal turnover rates ($v = 0.058$–0.106, $P < 0.014$) for fungi (Fig. 1b,d). In contrast, both bacteria and fungi exhibited significant ($P < 0.011$) TDRs under warming based on both taxonomic and phylogenetic diversity (Fig. 1). Permutation tests indicated that the slopes of TDRs based on all diversity metrics were significantly steeper under warming than control for bacteria ($v = 0.091$–0.101, $P < 0.001$) and fungi ($v = 0.134$–0.248, $P < 0.006$) (Fig. 1). Considerably steeper slopes of TDRs under warming were observed for bacteria with abundance-based metrics (Bray–Curtis and/or weighted UniFrac) and for fungi with Bray–Curtis (Supplementary Fig. 3a–c). However, such a trend was less obvious for fungi with weighted UniFrac (Supplementary Fig. 3d). Second, TDRs of different lineages of bacteria and fungi were also estimated at the phylum level based on taxonomic and phylogenetic diversity (Supplementary Tables 2 and 3). Different lineages in bacteria and fungi showed substantial variations of TDRs (up to tenfold) (Fig. 2 and Supplementary Fig. 4), particularly in control plots, which had fewer significant TDRs (10%) with relatively small or negative v; for example, *Chloroflexi* in bacteria (Fig. 2 and Supplementary Fig. 4). In contrast, significant positive v was observed under warming for most of these phyla based on both taxonomic and phylogenetic diversity metrics. For instance, the phyla *Actinobacteria* and *Proteobacteria* in bacteria showed no significant v under control conditions, but significant v was observed in these phyla under warming (Supplementary Tables 2 and 3). More importantly, the rates of time decay of community structure for most of these phyla (75%) under warming were significantly ($P < 0.10$) larger than those under control (Fig. 2 and Supplementary Fig. 4). Third, fungi exhibited a significantly ($P < 0.001$) larger slope of TDRs (1.5–4 times) than bacteria and archaea under warming (Fig. 1 and Supplementary Fig. 3), suggesting that experimental warming may have differential effects on the temporal succession of bacteria and fungi. In addition, the temporal turnovers of

microbial community composition and structure based on phylogenetic diversity metrics were significantly ($P < 0.001$) lower than those based on taxonomic diversity metrics for most bacterial and fungal lineages (Figs. 1 and 2), which could be because the experimental period (six years) was not sufficient to allow rapid phylogenetic divergences. Collectively, all of these results indicated that six years of experimental warming significantly accelerated the temporal turnover rates of soil bacteria and fungi, and these effects are also lineage dependent.

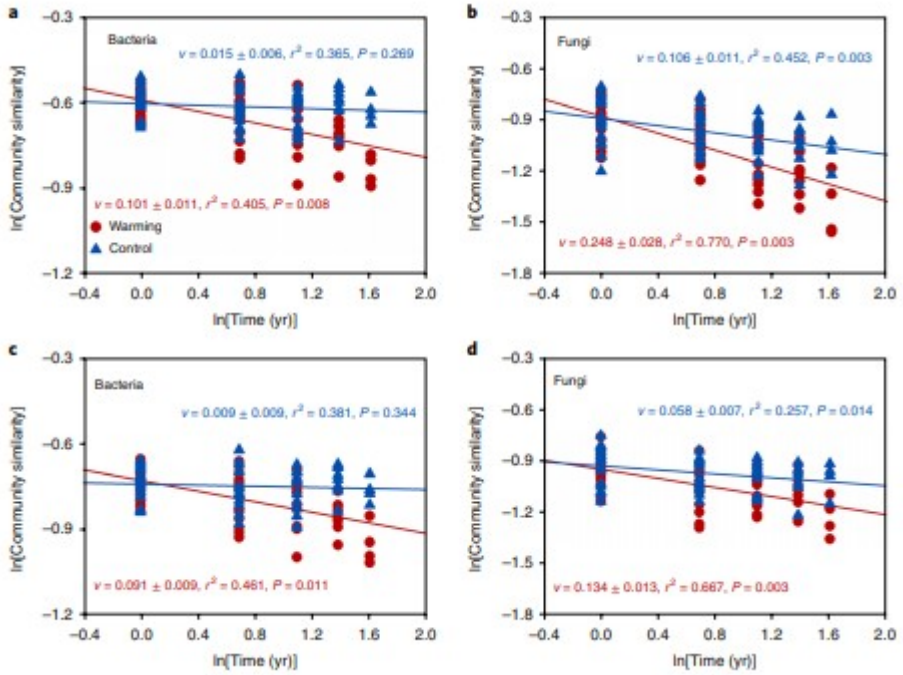

Fig. 1: The TDRs of fungal and bacterial communities under warming and control conditions. **a**,**b**, Taxonomic diversity. **c**,**d**, Phylogenetic diversity. Taxonomic diversity was measured by Sorensen and phylogenetic diversity was calculated as unweighted UniFrac. Considering the repeated-measures design, the logarithmic between-year similarity values at each plot were fitted to a linear mixed model (LMM) with a fixed effect of logarithmic time difference and a random intercept and slope effect among plots. The TDR values (v) are presented as a coefficient in fixed effect ± standard error in random effect. The r^2 values were calculated (details in Methods), reflecting variance explained by the whole LMM model. The P value of each TDR was based on a permutation test. The lines show the fixed effects in the LMM. Further permutation tests indicated that the TDR values (v) of both bacteria and fungi were significantly different ($P < 0.01$) between the warming treatment and control.

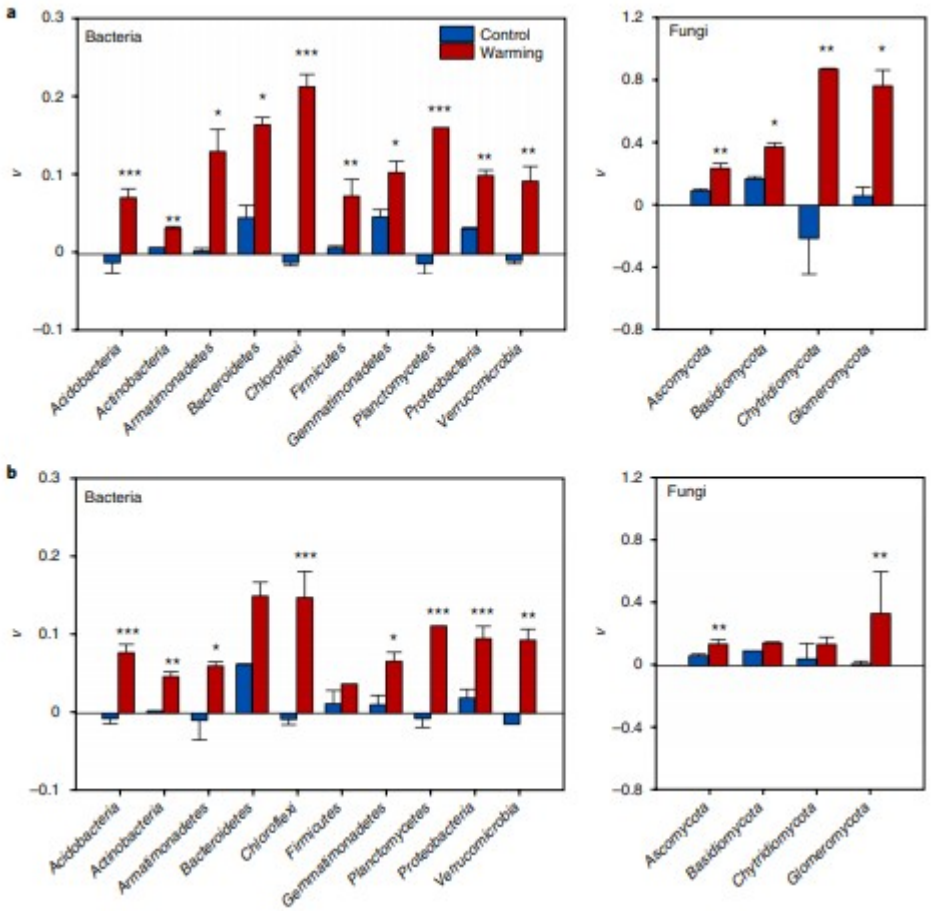

Fig. 2: TDR values of microbial communities among different phylogenetic groups under warming and control. **a**, Sorensen metrics. **b**, Unweighted UniFrac dissimilarity metrics. The TDR values in different phyla were calculated from a LMM as described in Fig. 1. The bars represent standard errors. The significance of the differences of TDR values between warming and control in each phylum was based on a permutation test and is indicated as $***P < 0.01$, $**P < 0.05$ and $*P < 0.10$. The information for other diversity metrics (Bray–Curtis and weighted UniFrac) is shown in Supplementary Fig. 4.

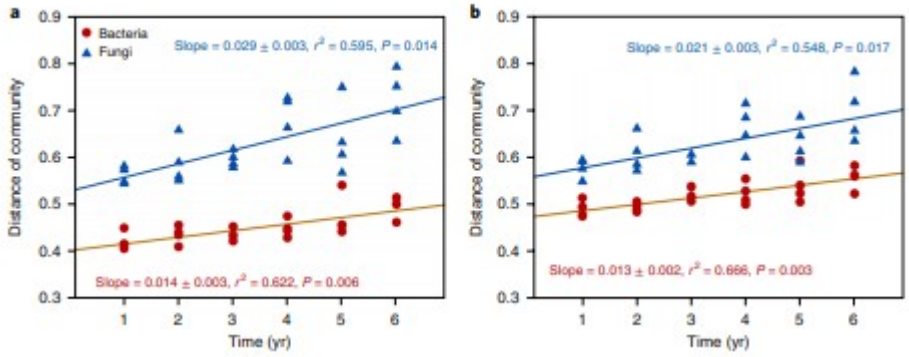

Fig. 3 | Temporal change in community differences between warming and control conditions. **a**, Sorensen metrics. **b**, Unweighted UniFrac dissimilarity metrics. Community distances of bacteria and fungi between warming and control increased

linearly with time. The first year is 2009. Considering the repeated-measures design, the warming-versus-control dissimilarity values at each block were fitted to LMMs with a fixed effect of time and a random intercept and slope effect among different pairs of plots (blocks). The slopes are presented as a coefficient in fixed effect ± standard error in random effect. The r 2 values are calculated (details in Methods), reflecting variance explained by the whole LMM model. *P* values were based on permutation tests. The lines showed the fixed effects of the LMM.

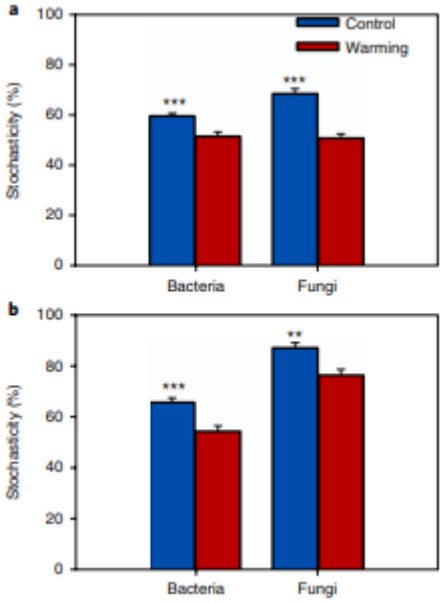

Fig. 4: Overall community stochasticity under warming and control conditions. **a**, Taxonomic (Sorensen) metrics. **b**, Phylogenetic (mean-nearest-taxon-distance) metrics. Warming significantly decreased the stochasticity of bacterial and fungal community assemblages. The significances of the community difference between warming and control are indicated as ***$P < 0.01$ and **$P < 0.05$ based on permutational multivariate analysis of variance with constraints related to the repeated-measures design. The error bars indicate standard errors.

To further determine how warming affects the succession of bacterial and fungal communities over time, differences of microbial communities between paired warmed and control plots were determined on a yearly basis. Our results first showed that the differences of bacterial and fungal community structure between warming and control all increased linearly with time based on Sorensen and unweighted UniFrac for bacteria (slope = 0.013–0.014, $P <$ 0.001) and fungi (slope = 0.021–0.029, $P < 0.001$) (Fig. 3). Similarly, the differences between warming and control based on Bray–Curtis and weighted UniFrac also exhibited an increase with time for bacteria and fungi, although the increases were not significant (Supplementary Fig. 5). The paired differences of different lineages between warmed and control plots were also evaluated (Supplementary Tables 4 and 5). Our results showed that over half of the bacterial and fungal phyla exhibited significantly or marginally significantly positive slopes of community difference between warming and control based on Sorensen and unweighted UniFrac dissimilarity metrics

(Supplementary Fig. 6). Positive slopes of community difference between warming and control were observed in most of the lineages based on Bray–Curtis and weighted UniFrac dissimilarity metrics (Supplementary Fig. 7). In addition, the paired differences of microbial communities between warmed and control plots were significantly ($P < 0.05$) larger in fungi than bacteria based on various metrics (Fig. 3), suggesting that warming could have bigger impacts on the temporal turnovers in fungi than bacteria. Significant correlations ($r = 0.507–0.803$, $P < 0.011$) of community difference were detected between bacterial and fungal communities under warming and control based on various metrics, except weighted UniFrac (Supplementary Fig. 8). Together, these results suggested that experimental warming significantly enhanced the divergent succession of soil bacterial and fungal communities.

The altered microbial successional dynamics could be caused by a variety of environmental factors other than warming. Canonical correspondence analysis (CCA) showed that composition and structure of bacteria and fungi were significantly ($F = 1.066–1.208$, $P < 0.05$) shaped by several common environmental variables, including GPP, ER, soil temperature, nutrients, moisture, pH and time (Supplementary Figs. 9 and 10). The variation of bacterial community was explained more by soil temperature ($r^2 = 0.425$, $P < 0.001$) than moisture ($r^2 = 0.159$, $P = 0.019$), but soil moisture ($r^2 = 0.153$, $P = 0.028$) explained higher variation of the fungal community than temperature ($r^2 = 0.100$, $P = 0.049$) (Supplementary Figs. 9 and 10). A partial Mantel test also indicated that temperature was a more important factor for bacterial community and most bacterial lineages, whereas soil moisture was more vital for fungal community and most fungal lineages (Supplementary Table 6). Furthermore, the CCA and Mantel test showed that the variations of microbial communities and their lineages significantly ($P < 0.05$) correlated with GPP, ER, TR and/or HR, suggesting that divergent succession of microbial communities under warming could affect certain ecosystem functions (Supplementary Tables 7 and 8). However, a partial CCA-based variation partitioning analysis indicated that relatively small portions (29.0–31.6%) of the variations in bacterial and fungal community composition and structure were explained by the environmental variables examined (Supplementary Figs. 9 and 10). Substantial portions of the community variations (68.4–71.0%) could not be explained by measured environmental variables, suggesting that stochastic processes[19,29] and/or unmeasured environmental variables could play more important roles than deterministic processes in the assembly of the soil bacterial and fungal communities.

To further discern the importance of stochastic processes in shaping the soil community structure, stochastic ratios[19] were calculated on the basis of taxonomic and phylogenetic metrics. After 6 years of warming, the stochastic processes contributed to considerable portions of the community variations under warming and control in taxonomic (50.6–68.1%) and phylogenetic (54.1–86.5%) diversity (Fig. 4). These results suggested that

stochastic processes could play more important roles in shaping microbial community structure, which is consistent with results from the variation partitioning analysis as described above. Interestingly, warming significantly ($P < 0.05$) decreased the relative importance of stochastic processes by 4.6–17.6% in shaping bacterial and fungal community structure (Fig. 4). Furthermore, the relative importance of stochastic processes in governing community structure decreased substantially over time under climate warming, particularly for bacteria (Supplementary Fig. 11). These results indicated that warming could act as a deterministic filtering factor to impose significant selection on microorganisms (for example, selecting microorganisms processing carbon faster for their growth) so that the overall community-level stochasticity decreased over time.

Our study demonstrates that warming played an important role in accelerating temporal turnover rates of soil bacterial and fungal communities. These results are consistent with a recent study showing that temperature plays a primary role in shaping microbial community diversity[30]. Our findings have important implications for predicting ecological consequences of climate warming. On one hand, since climate warming leads to microbial community divergence, microbial communities would be much more different from the contemporary community states under future climate change scenarios, and there is a higher likelihood that microbial communities will diverge towards multiple alternative community states. Consequently, the future successional trajectories in a warmed world will be less predictable based on the knowledge of contemporary communities. On the other hand, since warming reduced stochasticity over time, the communities could converge more quickly to a community state with less stochasticity under warming. Thus, if there is sufficient knowledge on the successional trajectories of the contemporary microbial communities, the microbial community composition and structure could be less variable under future climate warming. However, further research is needed to examine whether the warming-induced divergent succession and declining importance of stochastic processes identified in this study are applicable to other ecosystems.

Methods

Site description

This study was conducted at the Kessler Atmospheric and Ecological Field Station (KAEFS) in the US Great Plains in McClain County, Oklahoma (34° 59′ N, 97° 31′ W)[24]. KAEFS is an old-field tall-grass prairie abandoned from field cropping 40 years ago with light grazing until 2008. The grassland is dominated by C_3 forbs (*Ambrosia trifida*, *Solanum carolinense* and *Euphorbia dentate*) and C_4 grasses (*Tridens flavus*, *Sporobolus compositus* and *Sorghum halapense*)[24]. Based on Oklahoma Climatological Survey data from 1948 to 1999, the temperature ranges from 3.3 °C in January to 28.1 °C in July (mean annual temperature, 16.3 °C) and the precipitation ranges from

82 mm in January and February to 240 mm in May and June (mean annual precipitation, 914 mm)[2]. The soil type of this site is Port–Pulaski–Keokuk complex, which is a well-drained soil that is formed in loamy sediment on flood plains[25]. The soil texture class is loam with 51% of sand, 35% of silt and 13% of clay[25]. The concentrations of soil organic matter and total nitrogen (N) are 1.9% and 0.1%, respectively, and the soil bulk density is 1.2 g cm^{-3}. The soil has a high available water holding capacity (37%), neutral pH and a deep (about 70 cm), moderately penetrable root zone[24].

The field site experiment was established in July of 2009 with a blocked split-plot design, in which warming is a primary factor. Two levels of warming (ambient and +3°C) were set for four pairs of 2.5 m × 1.75 m plots by utilizing a ‘real’ or ‘dummy’ infrared radiator (Kalglo Electronics). In warmed plots, a real infrared radiator was suspended 1.5 m above the ground, and the dummy infrared radiator was suspended to simulate a shading effect of the device in the control plots.

Field measurements

Constantan-copper thermocouples wired to a Campbell Scientific CR10x data logger (Campbell Scientific) were used to measure and record soil temperature every 15 min at 7.5, 20, 45 and 75 cm in the centre of each plot. To represent the microclimate of the soil where the microbial communities were sampled, the soil temperature data used in this study were the annual average values at 7.5 cm depth across the whole year. Unfortunately, probes and data lines for measuring soil water content were destroyed by rodents in the beginning of field experiment. Instead, volumetric soil water content (%V) from the soil surface to a 15-cm depth was measured once or twice a month using a portable time domain reflectometer (Soil Moisture Equipment Corp.). Three measurements of soil moisture were performed in every plot and the average values were used in analyses. The soil moisture data presented in this study were annually averaged across each year.

Ecosystem carbon (C) fluxes were measured once or twice a month between 10:00 and 15:00 (local time) as described previously[2,24]. Net ecosystem exchange and ER were measured using an LI-6400 portable photosynthesis system (LI-COR) attached to a transparent chamber (0.5 m × 0.5 m × 0.7 m), which covered all of the vegetation within the aluminium frames[31]. GPP was estimated as the difference between net ecosystem exchange and ER. Meanwhile, soil TR and HR were measured using a LI-8100A soil flux system attached to a soil CO_2 flux chamber (LI-COR) as described previously[25]. Autotrophic respiration was estimated as the difference between TR and HR. The annual average values of ecosystem C fluxes and respirations across each year were used to represent the responses of grassland ecosystem in this study.

Above-ground plant community investigations were annually conducted at peak biomass (usually September) as described previously[24,32]. Above-ground plant biomass, separated into C_3 and C_4 species, was indirectly estimated by

a modified pin-touch method[24,32]. A detailed description of biomass estimation is provided by Sherry et al.[33]. All of the species within each plot were identified to estimate species richness. Since there was no carryover of living biomass from previous years due to a distinct dormant season, and negligible decomposition of biomass during the growing season in our ecosystem, the estimated above-ground plant biomass was considered to be above-ground net primary production.

Sampling and soil chemical measurements

In this study, 8 surface (0–15 cm) soil samples were collected annually in 4 control and 4 warmed plots at approximately the date of peak plant biomass (September or October) from 2009 to 2014. Three soil cores (2.5 cm diameter x 15 cm deep) were collected using a soil sampler tube and composited to have enough samples for soil chemistry, microbiology and molecular biology analyses. A total of 48 soil samples were analysed in this study.

Before microbial and chemical analyses, visible roots (>0.25 cm) and stones were removed from the soil by metal forceps. All soil samples were analysed by the Soil, Water, and Forage Analytical Laboratory at Oklahoma State University (Stillwater, OK, USA). The organic C and total N contents in soil were determined using a dry combustion C and N analyser (LECO). Soil nitrate (NO_3^-) and ammonia (NH_4^+) were analysed using a Lachat 8000 flow-injection analyser (Lachat). Soil pH was measured at a water-to-soil mass ratio of 2.5:1 using a pH meter with a calibrated combined glass electrode[34].

DNA extraction

Soil DNA was extracted from 1.5 g soil by freeze-grinding and SDS-based lysis as described previously[35], and purified with a MoBio PowerSoil DNA isolation kit (MoBio Laboratories) according to the manufacturer's protocol. DNA quality was assessed on the basis of 260/280 nm and 260/230 nm absorbance ratios using a NanoDrop ND-1000 Spectrophotometer (NanoDrop Technologies). The final DNA concentrations were quantified by PicoGreen using a FLUOstar Optima fluorescence plant reader (BMG Labtech). DNAs were stored at −80 °C until sequencing analysis.

Amplicon sequencing

Library construction and sequencing were processed using methods similar to those described in previous reports[36]. Universal primer sets, 515F (5′-GTGCCAGCMGCCGCGGTAA-3′) and 806R (5′-GGACTACHVGGGTWTCTAAT-3′) targeting the V3–V4 hypervariable region of bacterial and archaeal 16S rRNA genes[37], and gITS7F (5′-GTGARTCATCGARTCTTTG-3′) and ITS4R (5′-TCCTCCGCTTATTGATATGC-3′) for fungal ITSs between 5.8S and 28S rRNA genes[30], were used in this study. Library preparation was performed using a two-step PCR to avoid extra PCR bias as previously documented[10,36,38]. Phasing primers, which contained different-length spacers (0–7 bases) between the sequencing primer and the target gene to randomize base

position during sequencing[36], were designed and used in the second step of the two-step PCR. The forward and reverse primers were used in a complementary manner to ensure that the total length of the amplified sequences remained constant. Both forward and reverse phasing primers have the Illumina adaptor, the Illumina sequencing primer, a spacer, and the target gene primer and a barcode of 12 bases in the reverse primer between the sequencing primer and the adaptor. In the two-step PCR, soil DNA was first diluted to 2.5 ng μl^{-1} with water to be used as a template in the PCR reaction. The 25 µl PCR reaction system and conditions were described previously[30,36]. Reactions of 16S rRNA gene and ITS amplification were performed in triplicates. After amplification, the triplicate products were combined together, visualized by 1% agarose gel electrophoresis and quantified by PicoGreen using a FLUOstar Optima fluorescence plant reader (BMG Labtech).

PCR products from different samples were pooled at equal molality (generally <300 samples) to be sequenced in the same MiSeq run. The pooled mixture was purified with a QIAquick gel extraction kit (Qiagen Sciences) and re-quantified with PicoGreen. Sample libraries for sequencing were prepared according to the MiSeq Reagent Kit Preparation Guide (Illumina) as described previously[36,38]. The pooled sample library was diluted to 2 nM; 10 µl of 0.2 N fresh NaOH was then added into 10 µl of sample DNA for denaturation. The denatured DNA was diluted to 6 pM and mixed with an equal volume of 6 pM Phi X library. Finally, the mixture (600 µl) was loaded into a reagent cartridge and sequenced on a MiSeq (Illumina) using 2 × 250 pair-end sequencing kit by following manufacturer's instructions.

Sequence preprocessing

The raw reads of the 16S rRNA gene and ITS were collected by the MiSeq in fastq format, and then submitted to our data analysis website (http://zhoulab5.rccc.ou.edu:8080) to be further analysed using a sequence analysis pipeline built on the Galaxy platform[39]. After removing spiked PhiX reads, the reads were assigned into different sample libraries based on the barcodes. Primer sequences at the end of each read were trimmed and the Btrim program[40] with a threshold of QC > 20 over a 5-bp window size was used to filter the reads. For 16S and ITS, forward and reverse reads of the same sequence with at least 20 bp overlap and <5% mismatches were combined using FLASH[41]. Any joined sequences with an ambiguous base or a length of <245 bp for the 16S rRNA gene or <220 bp for the ITS were discarded. Thereafter, operational taxonomic units (OTUs) were clustered by UPARSE[42] at 97% identity and singletons were removed from the remaining sequences for both the 16S rRNA gene and the ITS. In UPARSE, the green reference data set[43] for 16S data and the UNITE/QIIME-released ITS reference data set (https://unite.ut.ee/repository.php) for ITS data were used as reference databases to remove chimaeras. To normalize samples to the same total read abundance, 30,000 sequences for the 16S rRNA gene and 10,000 sequences for the ITS were randomly selected (resampled) for each

sample. OTU taxonomic classification of the ITS and 16S rRNA gene sequences was performed using representative sequences from each OTU through the Ribosomal Database Project Classifier with 50% confidence estimates[44].

Sorensen and Bray–Curtis dissimilarity metrics were calculated to estimate taxonomic diversity based on the resampled OTU tables in R using the vegan package[45]. Weighted and unweighted UniFrac distances were calculated to estimate phylogenetic diversity of microbial communities in R using the phyloseq package[46]. These taxonomic and phylogenetic dissimilarity metrics were used to evaluate microbial TDR and succession rates in all subsequent analyses.

TDR and succession estimation

Similar to distance-decay relationships[27,47], the TDRs of microbial communities are usually evaluated using the similar linear regression between logarithmic β-similarities and logarithmic temporal distance in the following form (equation (1)).

$$\ln(S_s) = c - v\ln(T) + \varepsilon \qquad (1)$$

where S_s is the pairwise similarity in community composition, T is the time interval, the slope v is the TDR value, a measure of the temporal turnover rate of the community across time, c is the intercept and ε is the residuals.

In this study, we used the same moving window approach to assess time decay in microbial communities as previously described[27,47]. This approach involves partitioning a time series into different subset windows given the number of observations and fitting the TDR model. In our annual survey data, subset window 1 included the pairwise similarity of samples that were one year apart; subset window 2 is the pairwise similarity of samples two years apart, and so on. In our six-year record, there are 5 one-year intervals, 4 two-year intervals, 3 three-year intervals, down to 1 five-year interval for each plot. This moving window approach is currently the dominant approach for TDRs[47,48,49,50]. Considering the repeated-measures design, TDR analysis counted only pairwise comparisons among time points within each plot (that is, 15 pairwise comparisons for each plot and a total of 60 pairwise comparisons for each treatment).

In general, the above TDR model is fitted as a linear model, where the slope v and the intercept c are both constant across a data set. However, our experimental design has repeated measures at different time points in the same plot, and different plots under the same treatment do not necessarily have the same slope and intercept. Thus, we fitted the data for each treatment to the TDR model by an LMM rather than common linear model. To make the slope v and intercept c variable at different plots, each of them is divided into two parts (equations (2) and (3)). One part (λ_v and λ_c) is constant and contributes to the ‘fixed effect’ of the LMM (equation (4)), which

represents the average slope and intercept estimated across different plots. The other part (δ_v and δ_c) can have different values in different plots with a mean expectation of zero, contributing to the plot-specific 'random effect' of the LMM (equation (4)). The model was calculated using the function lmer in the R package lme4 with model setting as $\ln(S_s) \sim \ln(dT) + [1 + \ln(dT)]|\text{plot}$.

$$v = \lambda_v + \delta_v \quad (2)$$

$$c = \lambda_c + \delta_c \quad (3)$$

$$\ln(S_s) = (\lambda_c + \delta_c) - (\lambda_v + \delta_v)\ln(T) + \varepsilon = \underbrace{[\lambda_c - \lambda_v \ln(T)]}_{\text{Fixed effect}} + \underbrace{[\delta_c - \delta_v \ln(T)]}_{\text{Random effect}} + \varepsilon \quad (4)$$

To evaluate how the data can be explained by the TDR model, the coefficient of determination (r^2) was calculated for each LMM as described previously (named conditional R^2 in Nakagawa and Schielzeth's method)[26]. The significance of each LMM was calculated by a permutation test rather than a parametric test considering the dependence among the pairwise comparisons. The permutation test for the LMM randomized the 6 time points (years) for 720 times (complete enumeration), and the *P* value was calculated by comparing the Akaike information criterion of the observed LMM with the permuted ones. We also performed a permutation test to calculate the significance of the TDR value difference between warming and control[51]. The observed TDR value difference between warming and control was compared with the TDR value difference in permuted data sets to obtain the *P* value. For TDR analysis in each phylum, the relative abundance in each phylum was recalculated to reduce the dependence between phyla. Then, TDR values (v) and significance for each phylum were calculated as described above. To control the false discovery rate in multiple testing, the *P* values of different phyla were corrected by the method 'fdr' using the function 'p.adjust' in the R package 'stats'[52,53].

We evaluated the impacts of warming on the succession of soil bacterial and fungal communities using the distances of microbial communities between warming and control at each block in each year[27]. Such comparisons will potentially minimize, if not eliminate, the effects of experimental noise, due to annual sampling time differences, environmental fluctuations, molecular marker resolution and/or technical variation, on community temporal turnovers. At each time point, microbial communities in each warming plot were compared with the control plot in the same block, generating a total of four pairwise comparisons in each year. The difference between each pair of plots (D) was measured each year and the intercepts and slopes of temporal change between different pairs of plots are not necessarily the same; therefore, we fitted the temporal change to LMM with a random intercept and slope effect among different pairs of plots (blocks).

$$D = b + at + \varepsilon = (\lambda_b + \delta_b) + (\lambda_a + \delta_a)t + \varepsilon$$
$$= \underbrace{(\lambda_b + \lambda_a t)}_{\text{Fixed effect}} + \underbrace{(\delta_b + \delta_a t)}_{\text{Random effect}} + \varepsilon \quad (5)$$

where D is the dissimilarity between warming and control plots, t is the time (year), and both the slope a and intercept b have fixed (λ_a, λ_b) and variable (δ_a, δ_b) parts contributing to the fixed effect and block-specific random effect of the LMM.

The model was set as $D \sim t + (1 + t)|\text{Block}$, where D represents dissimilarity and t represents year. LMM, r^2_m, r^2_c and significance were calculated as described above. For succession analysis in each phylum, the relative abundance in each phylum was recalculated to reduce the dependence between phyla. Then, the slope of community difference and the significance for each phylum were obtained as described above. The P values of different phyla were corrected as described above.

Stochastic community assembly

Beta-diversity indices can provide insights into community assembly mechanisms[54]. To disentangle the importance of deterministic mechanisms from stochastic mechanisms underlying community assembly, a null model analysis reported by Chase et al.[54] was used based on both taxonomic (Sorensen) and phylogenetic (beta-mean-nearest-taxon-distance[55]) metrics. To evaluate the relative importance of stochastic processes in shaping community structure, the stochastic ratio was calculated using the modified method as previously described[19]. Since the taxonomic and phylogenetic metrics were originally derived from every pairwise comparison, they may not be independent. Therefore, we performed permutational multivariate analysis of variance with some modification considering our hypothesis and the repeated-measures design. We hypothesized that the stochasticity in community turnover among warming plots could be significantly different from that among control plots. Thus, the treatment (warming versus control) was permuted within each block in each year rather than freely randomized across years. In all randomized and observed data sets, we counted the pairwise stochasticity values within each treatment in each year and compared the within-warming stochasticity to the within-control stochasticity. The F value was calculated with ‘block’ and ‘year’ as constraints; that is, stochasticity ~ warming + Error(block × year). The P value was calculated by comparing the observed F value with those from 1,000 randomized data sets.

Statistical analysis

Various statistical analyses were carried out using R software 3.1.1 with the package vegan (v.2.3-5) unless otherwise indicated. Difference of soil variables, plant characteristics and ecosystem functions between warming and control was compared by repeated-measures analysis of variance (ANOVA). The microbial temporal patterns under warmed and control plots

were determined by non-metric multidimensional scaling ordination based on the Bray–Curtis dissimilarity[56]. Three different non-parametric multivariate statistical tests (non-parametric multivariate analysis of variance (Adonis), analysis of similarity (ANOSIM) and multi-response permutation procedure (MRPP)) were used to test the differences in soil microbial communities under warming and control treatments[2]. For Adonis, the one-way repeated-measures ANOVA model was set as 'dissimilarity ~ warming + block × year' when using the function Adonis in the R package vegan. For ANOSIM and MRPP, the permutation was constrained within each block in each year by setting 'strata' in the functions ANOSIM and MRPP in the R package vegan. CCA was performed to determine the linkage between ecosystem functional parameters and microbial community structures. The function envfit in the R package vegan was used to evaluate the association of microbial community variation and each environmental variable in CCA. The significance of the CCA model was tested using ANOVA. Based on CCA results, variation partitioning analysis was performed to determine the contributions of each individual variable or groups of variables to total variations in the soil microbial community composition. Mantel and partial Mantel tests were also performed to calculate the correlations between environmental factors and soil microbial communities.

Data availability

DNA sequences of 16S rRNA gene and ITS amplicons are available in the NCBI Sequence Read Archive under project no. PRJNA331185.

Acknowledgements

This work is supported by the US Department of Energy, Office of Science, Genomic Science Program under award numbers DE-SC0004601 and DE-SC0010715, the National Science Foundation of China (no. 41430856) and the Office of the Vice President for Research at the University of Oklahoma. X.G. and X.Z. were generously supported by the China Scholarship Council (CSC).

References

1. IPCC Climate Change 2013: The Physical Science Basis (eds Stocker, T. F. et al.) (Cambridge Univ. Press, 2013).

2. Zhou, J. et al. Microbial mediation of carbon-cycle feedbacks to climate warming. Nat. Clim. Change 2, 106–110 (2012).

3. Heimann, M. & Reichstein, M. Terrestrial ecosystem carbon dynamics and climate feedbacks. Nature 451, 289–292 (2008).

4. Van Der Gast, C. J., Ager, D. & Lilley, A. K. Temporal scaling of bacterial taxa is influenced by both stochastic and deterministic ecological factors. Environ. Microbiol. 10, 1411–1418 (2008).

5. Adler, P. B. & Lauenroth, W. K. The power of time: spatiotemporal scaling of species diversity. Ecol. Lett. 6, 749–756 (2003).

6. Brown, J. H., Gillooly, J. F., Allen, A. P., Savage, V. M. & West, G. B. Toward a metabolic theory of ecology. Ecology 85, 1771–1789 (2004).

7. Chen, I. C., Hill, J. K., Ohlemuller, R., Roy, D. B. & Tomas, C. D. Rapid range shifts of species associated with high levels of climate warming. Science 333, 1024–1026 (2011).

8. Sherry, R. A. et al. Divergence of reproductive phenology under climate warming. Proc. Natl Acad. Sci. USA 104, 198–202 (2007).

9. Berg, M. P. et al. Adapt or disperse: understanding species persistence in a changing world. Glob. Change Biol. 16, 587–598 (2010).

10. Xue, K. et al. Tundra soil carbon is vulnerable to rapid microbial decomposition under climate warming. Nat. Clim. Change 6, 595–600 (2016).

11. Cardinale, B. J. et al. Biodiversity loss and its impact on humanity. Nature 486, 59–67 (2012).

12. Bebber, D. P., Ramotowski, M. A. & Gurr, S. J. Crop pests and pathogens move polewards in a warming world. Nat. Clim. Change 3, 985–988 (2013).

13. Sistla, S. A. et al. Long-term warming restructures Arctic tundra without changing net soil carbon storage. Nature 497, 615–618 (2013).

14. Prach, K. & Walker, L. R. Four opportunities for studies of ecological succession. Trends Ecol. Evol. 26, 119–123 (2011).

15. Walker, L. R. & Del Moral, R. Primary Succession and Ecosystem Rehabilitation (Cambridge Univ. Press, Cambridge, 2003).

16. Li, S. P. et al. Convergence and divergence in a long-term old-field succession: the importance of spatial scale and species abundance. Ecol. Lett. 19, 1101–1109 (2016).

17. Fukami, T., Martijn Bezemer, T., Mortimer, S. R. & Putten, W. H. Species divergence and trait convergence in experimental plant community assembly. Ecol. Lett. 8, 1283–1290 (2005).

18. Inouye, R. S. & Tilman, D. Convergence and divergence of old-field vegetation after 11 yr of nitrogen addition. Ecology 76, 1872–1887 (1995).

19. Zhou, J. et al. Stochasticity, succession, and environmental perturbations in a fluidic ecosystem. Proc. Natl Acad. Sci. USA 111, E836–E845 (2014).

20. Schleicher, A., Peppler-Lisbach, C. & Kleyer, M. Functional traits during succession: is plant community assembly trait-driven? Preslia 83, 347–370 (2011).

21. Maignien, L., DeForce, E. A., Chafee, M. E., Eren, A. M. & Simmons, S. L. Ecological succession and stochastic variation in the assembly of Arabidopsis thaliana phyllosphere communities. MBio 5, e00682-13 (2014).

22. Veach, A. M., Stegen, J. C., Brown, S. P., Dodds, W. K. & Jumpponen, A. Spatial and successional dynamics of microbial biofilm communities in a grassland stream ecosystem. Mol. Ecol. 25, 4674–4688 (2016).

23. Nemergut, D. R. et al. Decreases in average bacterial community rRNA operon copy number during succession. ISME J. 10, 1147–1156 (2016).

24. Xu, X., Sherry, R. A., Niu, S., Li, D. & Luo, Y. Net primary productivity and rain-use efficiency as affected by warming, altered precipitation, and clipping in a mixed-grass prairie. Glob. Change Biol. 19, 2753–2764 (2013).

25. Li, D., Zhou, X., Wu, L., Zhou, J. & Luo, Y. Contrasting responses of heterotrophic and autotrophic respiration to experimental warming in a winter annual-dominated prairie. Glob. Change Biol. 19, 3553–3564 (2013).

26. Nakagawa, S. & Schielzeth, H. A general and simple method for obtaining R2 from generalized linear mixed-effects models. Methods Ecol. Evol. 4, 133–142 (2013).

27. Chen, L.-x et al. Comparative metagenomic and metatranscriptomic analyses of microbial communities in acid mine drainage. ISME J. 9, 1579–1592 (2015).

28. Webb, C. O., Ackerly, D. D., McPeek, M. A. & Donoghue, M. J. Phylogenies and community ecology. Annu. Rev. Ecol. Syst. 33, 475–505 (2002).

29. Zhou, J. & Ning, D. Stochastic community assembly: does it matter in microbial ecology? Microbiol. Mol. Biol. Rev. 81, e00002-17 (2017).

30. Zhou, J. et al. Temperature mediates continental-scale diversity of microbes in forest soils. Nat. Commun. 7, 12083 (2016).

31. Niu, S. et al. Water-mediated responses of ecosystem carbon fluxes to climatic change in a temperate steppe. New Phytol. 177, 209–219 (2008).

32. Frank, D. A. & McNaughton, S. J. Aboveground biomass estimation with the canopy intercept method: a plant growth form caveat. Oikos 57, 57–60 (1990).

33. Sherry, R. A. et al. Lagged effects of experimental warming and doubled precipitation on annual and seasonal aboveground biomass production in a tallgrass prairie. Glob. Change Biol. 14, 2923–2936 (2008).

34. McLean, E. O. in Methods of Soil Analysis. Part 2: Chemical and Microbiological Properties (ed. Page, A. L.) 199–224 (Soil Science Society of America, Madison, WI, 1982).

35. Zhou, J., Bruns, M. A. & Tiedje, J. M. DNA recovery from soils of diverse composition. Appl. Environ. Microbiol. 62, 316–322 (1996).

36. Wu, L. et al. Phasing amplicon sequencing on Illumina Miseq for robust environmental microbial community analysis. BMC Microbiol. 15, 125 (2015).

37. Peifer, J. A. et al. Diversity and heritability of the maize rhizosphere microbiome under field conditions. Proc. Natl Acad. Sci. USA 110, 6548–6553 (2013).

38. Caporaso, J. G. et al. Ultra-high-throughput microbial community analysis on the Illumina HiSeq and MiSeq platforms. ISME J. 6, 1621–1624 (2012).

39. Giardine, B. et al. Galaxy: a platform for interactive large-scale genome analysis. Genome Res. 15, 1451–1455 (2005).

40. Kong, Y. Btrim: a fast, lightweight adapter and quality trimming program for next-generation sequencing technologies. Genomics 98, 152–153 (2011).

41. Magoč, T. & Salzberg, S. L. FLASH: fast length adjustment of short reads to improve genome assemblies. Bioinformatics 27, 2957–2963 (2011).

42. Edgar, R. C. UPARSE: highly accurate OTU sequences from microbial amplicon reads. Nat. Methods 10, 996–998 (2013).

43. DeSantis, T. Z. et al. Greengenes, a chimera-checked 16S rRNA gene database and workbench compatible with ARB. Appl. Environ. Microbiol. 72, 5069–5072 (2006).

44. Wang, Q., Garrity, G. M., Tiedje, J. M. & Cole, J. R. Naive Bayesian classifier for rapid assignment of rRNA sequences into the new bacterial taxonomy. Appl. Environ. Microbiol. 73, 5261–5267 (2007).

45. Dixon, P. VEGAN. a package of R functions for community ecology. J. Veg. Sci. 14, 927–930 (2009).

46. McMurdie, P. J. & Holmes, S. phyloseq: an R package for reproducible interactive analysis and graphics of microbiome census data. PloS ONE 8, e61217 (2013).

47. Shade, A., Gregory Caporaso, J., Handelsman, J., Knight, R. & Fierer, N. A meta-analysis of changes in bacterial and archaeal communities with time. ISME J. 7, 1493–1506 (2013).

48. Liang, Y. et al. Long-term soil transplant simulating climate change with latitude significantly alters microbial temporal turnover. ISME J. 9, 2561–2572 (2015).

49. Nekola, J. C. & White, P. S. The distance decay of similarity in biogeography and ecology. J. Biogeogr. 26, 867–878 (1999).

50. Deng, Y. et al. Elevated carbon dioxide accelerates the spatial turnover of soil microbial communities. Glob. Change Biol. 22, 957–964 (2016).

51. Martiny, J. B., Eisen, J. A., Penn, K., Allison, S. D. & Horner-Devine, M. C. Drivers of bacterial β-diversity depend on spatial scale. Proc. Natl Acad. Sci. USA 108, 7850–7854 (2011).

52. Benjamini, Y. & Hochberg, Y. Controlling the false discovery rate: a practical and powerful approach to multiple testing. J. R. Stat. Soc. B, 289–300 (1995).

53. R Development Core Team R: A Language and Environment for Statistical Computing (R Foundation for Statistical Computing, 2011).

54. Chase, J. M. & Myers, J. A. Disentangling the importance of ecological niches from stochastic processes across scales. Phil. Trans. R. Soc. B 366, 2351–2363 (2011).

55. Stegen, J. C., Lin, X., Konopka, A. E. & Fredrickson, J. K. Stochastic and deterministic assembly processes in subsurface microbial communities. ISME J. 6, 1653–1664 (2012).

56. Kruskal, J. B. Nonmetric multidimensional scaling: a numerical method. Psychometrika 29, 115–129 (1964).